Error Corrections for Ultrawideband Ranging

Juri Sidorenko, Volker Schatz, Norbert Scherer-Negenborn, Michael Arens, and Urs Hugentobler

***Abstract*— Precise indoor localization is a major challenge in the field of localization. In this article, we investigate multiple error corrections for the ultrawideband (UWB) technology, in particular the DecaWave DW1000 transceiver. Both the time-of-arrival (TOA) and the time-difference-of-arrival (TDOA) methods are considered. Various clock-drift correction methods for TOA from the literature are reviewed and compared experimentally. The best performing method is extended to TDOA, corrections for the signal power dependence and the hardware delay are added, and two additional enhancements suggested. These are compared with each other and TOA in positioning experiments.**

***Index Terms*— DecaWave, time difference of arrival (TDOA), time of arrival (TOA), two-way ranging (TWR), ultrawideband (UWB).**

NOMENCLATURE

ADS-TWR	Asymmetric double-sided TWR.
AltDS-TWR	Alternative double-sided TWR.
BS	Base station.
CCSS-TWR	CFO-corrected TWR.
CFO	Carrier frequency offset.
ID	Identification number.
PLL	Phase-locked loop.
RF	Radio frequency.
SDS-TWR	Symmetric double-sided TWR.
SMD	Surface-mounted device.
SS-TWR	Single-sided TWR.
TDOA	Time difference of arrival.
TOA	Time of arrival.
TWR	Two-way ranging.
UWB	Ultrawideband.

mds
September 04, 2019

Manuscript received April 6, 2020; accepted May 12, 2020. Date of publication May 22, 2020; date of current version October 9, 2020. The Associate Editor coordinating the review process was Alessio De Angelis. *(Corresponding author: Juri Sidorenko.)*

Juri Sidorenko is with the Fraunhofer Institute of Optronics, System Technologies and Image Exploitation IOSB, 76275 Ettlingen, Germany, and also with the Institute of Astronomical and Physical Geodesy, Technical University of Munich, 80333 Munich, Germany (e-mail: juri.sidorenko@iosb.fraunhofer.de).

Volker Schatz, Norbert Scherer-Negenborn, and Michael Arens are with the Fraunhofer Institute of Optronics, System Technologies and Image Exploitation IOSB, 76275 Ettlingen, Germany.

Urs Hugentobler is with the Institute of Astronomical and Physical Geodesy, Technical University of Munich, 80333 Munich, Germany.

Digital Object Identifier 10.1109/TIM.2020.2996706

I. INTRODUCTION

LOCALIZATION systems have become indispensable in everyday life. Satellite navigation [1], [2] has replaced article maps and is now essential for self-driving cars. As the requirements of logistics and manufacturing processes increase, access to precise positional information is becoming a necessity. Depending on the operating conditions for the localization application, different measurement principles [3]–[5] and techniques [6]–[8] are available. Two of the most common measurement techniques are based on the TOA [6] and the TDOA [7]. TOA calculates the distance between two stations from the signal traveling time, whereas TDOA considers the travel time differences between the stations. The measuring equipment is just as important as the measurement technique itself. This article focuses on indoor RF-based localization systems. In general, indoor positioning applications are a challenge for RF-based localization systems. Reflections can generate interference with the main signal and lead to fading. Compared with narrowband signals, UWB signals are more robust against fading [9], [10]. The DecaWave transceiver [11] uses UWB technology and is compliant with the IEEE802.15.4-2011 standard [12]. It supports six frequency bands with the center frequencies from 3.5 to 6.5 GHz and data rates of up to 6.8 Mb/s. Depending on the selected center frequency, the bandwidth ranges from 500 to 1000 MHz. The precision and accuracy of the DecaWave UWB depend primarily on three factors: the clock drift, the received signal power, and hardware delay.

In the first part of this article, it is shown which TWR protocol is most suitable for correcting the effect of the clock drift. The results are then verified by experiments with the DecaWave UWB system.

Section II deals with the extension of the best TWR protocol for the TDOA application. In [13], it was shown how the signal power correction curve can be obtained automatically for every station individually. In the present publication, we demonstrate how to apply these corrections for TOA and TDOA localization. Section VI describes how a synchronization signal from the reference station can be used to perform a range measurement between the reference station and a tag for every TDOA position estimation. This information increases the number of equations and also allows us to estimate the time offset between the reference station and the tag. Table I presents the notations used in this article.

A. Contribution

In this article, we review the most common TWR protocols and present their residual error. Section II deals with the evaluation of these protocols by practical experiments. The

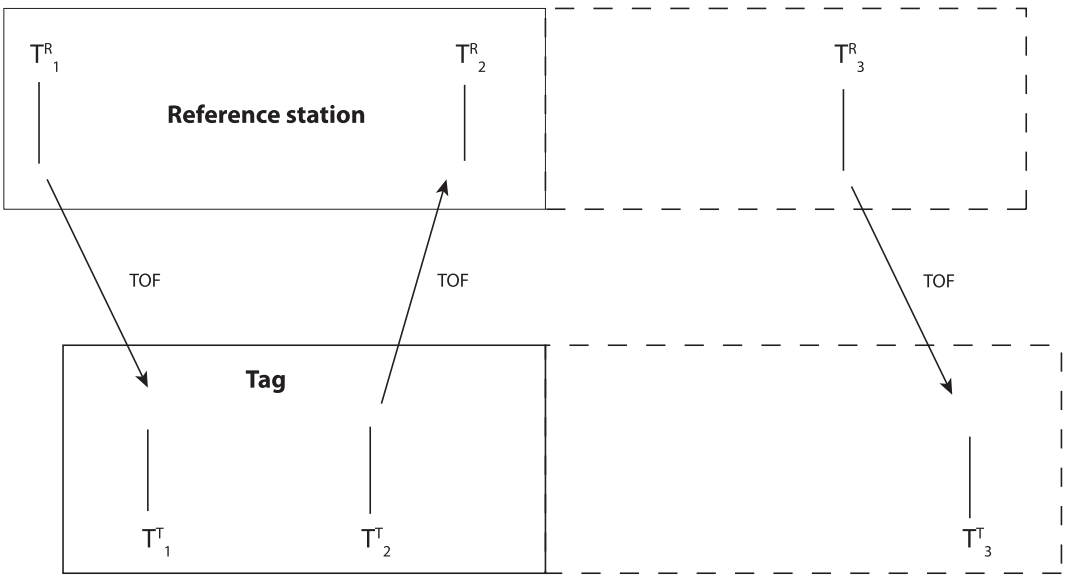

Fig. 1. TWR in theory.

TABLE I
NOTATIONS USED

Notation	Definition
A, B, C	Hardware delay
A_L	Linear parameter of the correction function
A_Q	First non-linear parameter of the correction function
B_Q	Second non-linear parameter of the correction function
$C_{n,m}$	Clock drift error, calculated from the timestamps n and m
F_C	Used clock drift error function correction term
F_L	Linear clock drift error function correction term
F_Q	Quadratic clock drift error function correction term
ϵ_{TWR}	Residual error
e_R	Frequency offset of the reference station (R.)
e_T	Frequency offset of the tag (T.)
$e_R - e_T$	Clock drift between the stations R. and T.
E	Timestamp error due to the signal power
K	Sending time difference between R. and T.
T_i^R	Timestamp at R.
T_i^T	Timestamp at T.
T_i^S	Timestamp at the anchor station S
$\Delta T_{n,m}$	Difference between two timestamps $T_m - T_n$
T_{TWR}	Time of flight without frequency drift
$\hat{T}_{TWR}$	Time of flight with frequency drift
T_{TOA}	Our TOA approach
T_{TDOA}	Our TDOA approach
T_{TDOA_K}	Our TDOA approach with the offset K
TWR	Index standing for the used TWR protocol
Z	Auxiliary results

best TWR protocol is extended by the ability to use the signal power and hardware delay correction for every station individually. In previous works, it was only possible to use the signal power correction for two stations after the ranging.

The second part of this article combines the findings from the TWR part to create a robust TDOA approach. We successively present our own TDOA solution; it has an additional range measurement and does not require computation of the unknown time offset between the reference station and the tag.

II. TOA MEASUREMENT TECHNIQUE

The TOA measurement technique provides the distance between two stations from the signal traveling time. In a one-way-ranging application, it is necessary that both stations are time synchronous. This condition can be bypassed if TWR is used instead. Fig. 1 shows the concept of TWR between two stations, with two and three messages. The initial station, also called the reference station, emits a signal at the local time T_1^R. The second station, named tag, receives the signal at its local time T_1^T and sends a response at its time T_2^T back to the reference station. The double time of flight can now be obtained by subtracting the delay of the second station $\Delta T_{1,2}^T = (T_2^T - T_1^T)$ from the transmitting and receiving time difference of the reference station $\Delta T_{1,2}^R = (T_2^R - T_1^R)$. Equation (1) shows the time of flight provided by the ideal TWR protocol

$$\text{TOF} = 0.5 \cdot \left(\Delta T_{1,2}^R - \Delta T_{1,2}^T\right). \tag{1}$$

In practice, the frequencies of the crystals are not identical, and small imperfections lead to the clock of one station operating faster or slower than the other. Since the TWR and the hardware become more commonly used, different approaches have been proposed to deal with the clock drift. Some of them, such as SS-TWR and CCSS-TWR, use two messages, whereas others require a third message, as shown in Fig. 1. In this section, the most common clock drift correction methods are analyzed in detail. We use the term clock drift error to refer to the integral of the clock drift. This error appears as the result of the clock drift and increases over time. We define that e_R and e_T denote the clock frequency offset of the reference station and tag, respectively. In the following, it is assumed that the frequency drift is constant during the ranging.

A. Single-Sided Two-Way Ranging

The SS-TWR protocol is the basic protocol without the clock drift correction. Hence, the time of flight is shown in the following equation:

$$T_{\text{SS}} = 0.5 \cdot \left(\Delta T_{1,2}^R - \Delta T_{1,2}^T\right). \tag{2}$$

The time of flight with the frequency offsets is presented in the following equation:

$$\hat{T}_{\mathrm{SS}} = 0.5 \cdot \left(\Delta T_{1,2}^{R}(1+e_R) - \Delta T_{1,2}^{T}(1+e_T)\right). \quad (3)$$

The residual error $\epsilon_{\mathrm{SS}} = \hat{T}_{\mathrm{SS}} - T_{\mathrm{SS}}$ is the error caused by the frequency offset. Equation (4) states that the residual error depends mainly on the response time of the tag, $\Delta T_{1,2}^{T}$. Even if the clock difference is just few parts per million (ppm) are delays $\Delta T_{1,2}^{T}$ in order of some milliseconds long, hence the multiplication leads to a significant impact on the range estimation. The clock drift error caused by the time of flight T_{SS} can be neglected, due to the short-range limitations of the UWB system

$$\epsilon_{\mathrm{SS}} = T_{\mathrm{SS}} e_R + 0.5 \cdot \Delta T_{1,2}^{T} \cdot (e_R - e_T). \quad (4)$$

B. CFO-(Corrected Single-Sided Two-Way Ranging)

Minimization of the residual error can be achieved by reducing the response time $\Delta T_{1,2}^{T}$ and using precise crystals. However, due to the real-life limitation, this is not always possible. In [17], a so-called CFO SS-TWR protocol was presented. It used the integrator of the PLL to obtain the clock drift difference between two DecaWave UWB transceivers. The information provided by the integrator of the PLL allows us to compensate for the effect of the clock drift during the message exchange. The residual error is computed as follows:

$$\epsilon_{\mathrm{CCSS}} = T_{\mathrm{CCSS}} \cdot e_R. \quad (5)$$

The residual error is now independent of the response time, and only the time of flight T_{CCSS} is the limiting factor. This technique is widely used in the community [18]–[20]. The reason why we will not use this method later on is that in [13], we showed that the integrator of the PLL depends on the signal power and therefore introduces additional inaccuracies.

C. Symmetric Double-Sided Two-Way Ranging

The SDS-TWR protocol [21] is part of the 802.15.4a standard. It was also introduced to minimize the errors due to crystal imperfections. In contrast to the previously presented CCSS-TWR method, three messages are now required, as shown in Fig. 1. With $\Delta T_{2,3}^{R} = (T_3^R - T_2^R)$ and $\Delta T_{2,3}^{T} = (T_3^T - T_2^T)$, the time of flight with the SDS-TWR protocol is obtained by the following equation:

$$T_{\mathrm{SDS}} = 0.25 \cdot \left(\Delta T_{1,2}^{R} - \Delta T_{1,2}^{T} + \Delta T_{2,3}^{T} - \Delta T_{2,3}^{R}\right). \quad (6)$$

The time of flight with the frequency offsets is shown in the following equation:

$$\hat{T}_{\mathrm{SDS}} = 0.25 \cdot \left(\Delta T_{1,2}^{R} - \Delta T_{2,3}^{R}\right)(1+e_R) + 0.25 \cdot \left(\Delta T_{2,3}^{T} - \Delta T_{1,2}^{T}\right)(1+e_T). \quad (7)$$

The residual error for the SDS-TWR is obtained analogously to SS-TWR, $\epsilon_{\mathrm{SDS}} = \hat{T}_{\mathrm{SDS}} - T_{\mathrm{SDS}}$. This leads to (8)

$$\epsilon_{\mathrm{SDS}} = 0.5 \cdot T_{\mathrm{SDS}}(e_R + e_T) + 0.25 \cdot \left(\Delta T_{1,2}^{T} - \Delta T_{2,3}^{R}\right) \cdot (e_R - e_T). \quad (8)$$

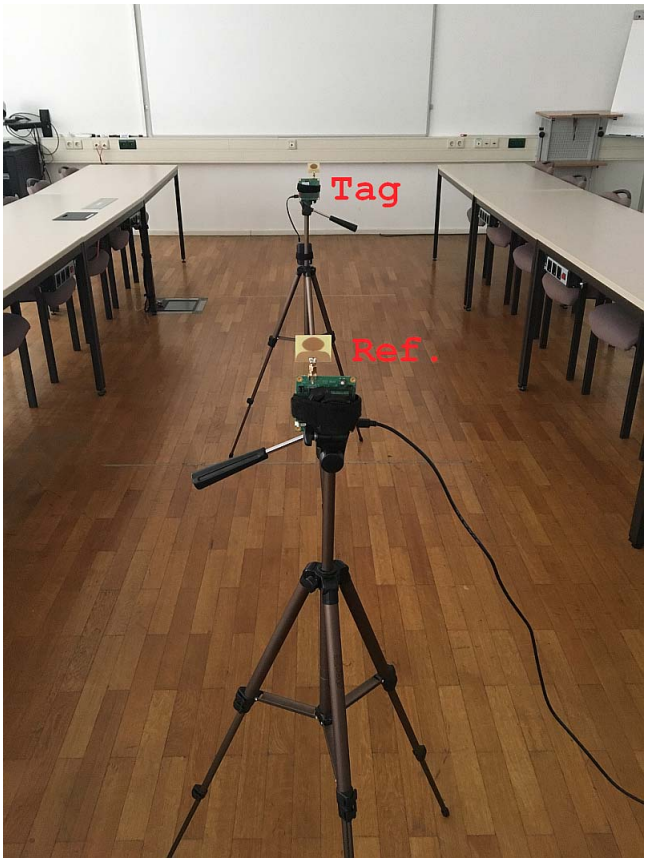

Fig. 2. Experimental setup of two DecaWave EVK1000 transceivers.

Again, it is possible to neglect the error caused by the time of flight. Therefore, the residual error of the SDS-TWR protocol depends mainly on the difference between the response time $\Delta T_{1,2}^{T}$ and $\Delta T_{2,3}^{R}$. In contrast to the CCSS-TWR protocol, the information about the clock drift is not used to correct the ranging, and it is more of an averaging.

D. Asymmetric Double-Sided Two-Way Ranging

The ADS-TWR protocol [22] is also often used in the field of localization. In general, it is an SDS-TWR protocol with the additional constraint that the response time $\Delta T_{2,3}^{R}$ is zero. This can be only achieved if the reference station sends the ranging message back to the tag instantly. The residual error is shown in the following equation:

$$\epsilon_{\mathrm{ADS}} = 0.5 \cdot T_{\mathrm{ADS}}(e_R + e_T) + 0.25 \cdot \left(\Delta T_{1,2}^{T}\right) \cdot (e_R - e_T). \quad (9)$$

E. Alternative Double-Sided Two-Way Ranging (AltDS-TWR)

The AltDS-TWR protocol [23] uses the fact that the time differences of the first and last message should be the same for the transmitter and for the receiver $\Delta T_{1,3}^{T}(1+e_T) = \Delta T_{1,3}^{R}(1+e_R)$. The deviation between both time differences represents the clock drift error. This error can be linearly interpolated to correct the time difference $\Delta T_{1,2}^{T}$. The time

of flight for the AltDS-TWR protocol is presented in the following equation:

$$T_{\mathrm{AltDS}} = \frac{\Delta T_{1,2}^{R} \cdot \Delta T_{2,3}^{T} - \Delta T_{1,2}^{T} \cdot \Delta T_{2,3}^{R}}{2\left(\Delta T_{2,3}^{T} + \Delta T_{1,2}^{T}\right)}. \tag{10}$$

The time of flight with the frequency offsets is presented in in the following equation:

$$\hat{T}_{\mathrm{AltDS}} = (1 + e_R)\frac{\Delta T_{1,2}^{R} \cdot \Delta T_{2,3}^{T} - \Delta T_{1,2}^{T} \cdot \Delta T_{2,3}^{R}}{2\left(\Delta T_{2,3}^{T} + \Delta T_{1,2}^{T}\right)}. \tag{11}$$

The residual error for the AltDS-TWR with $\epsilon_{\mathrm{AltDS}} = \hat{T}_{\mathrm{AltDS}} - T_{\mathrm{AltDS}}$ equates

$$\epsilon_{\mathrm{AltDS}} = e_R T_{\mathrm{AltDS}}. \tag{12}$$

The remaining error depends, equivalently to the CCSS-TWR protocol, on the time of flight. In some publications, the AltDS-TWR distance is presented as in (13). It should be noted that this equation applies only if $\Delta T_{1,3}^{T} = \Delta T_{1,3}^{R}$, which means without clock drift between the stations

$$T_{\mathrm{AltDS}} = \frac{\Delta T_{1,2}^{R} \cdot \Delta T_{2,3}^{T} - \Delta T_{1,2}^{T} \cdot \Delta T_{2,3}^{R}}{\left(\Delta T_{1,2}^{R} + \Delta T_{2,3}^{T} + \Delta T_{1,2}^{T} + \Delta T_{2,3}^{R}\right)}. \tag{13}$$

III. Experimental Results: Two-Way Ranging

In this section, the previously introduced residual errors due to clock drift between two stations are verified by practical measurements. The experimental setup is presented in Fig. 2. In each of the presented variants, the distance between stations was 1.5 m, with a measuring time of 30 min. The filtered values are, if not otherwise mentioned, using a moving average filter with a filter size of 500 measurements and an update rate of 25 measurements per second. This size was selected to remove the noise but preserve variations from the scale of a few milliseconds. It should be noted that the best result is a straight line, which means that the measured distance between the stations is always the same. The difference between the measurement and the expected 1.5 m is irrelevant for evaluating the clock drift correction, and it is just important that this offset is constant. In experiment, one and two are the results of the different ranging protocols based on the same measurement.

The ADS-TWR is not part of the upcoming plots since a zero response time is not feasible with our setup where response transmissions are triggered with a microcontroller external to the wireless transceiver. Even with the minimum possible response time, the distance determined with ADS-TWR is orders of magnitude larger than in reality.[1] However, we investigate the influence of the response time in Section III-A.

A. First TWR Experiment: TWR With Different Ranging Protocols

In this experiment, the response times of both stations were set to be as close to each other as possible: $T_{1,2}^{T} = 1.5566\,\mathrm{ms}$ and $T_{2,3}^{R} = 1.5530\,\mathrm{ms}$. In Fig. 3, the results of the different TWR protocols are presented. It can be observed that the uncorrected SS-TWR has the highest change in distance over time. This curve is the warm-up process of the system [15]. The difference between the SDS-TWR and AltDS-TWR is on average 0.2331 mm. The results of the SDS-TWR are hidden by the AltDS-TWR. This changes for the next experiment.

B. Second TWR Experiment: Dependence on the Response Time

In this experiment, the response delay $T_{1,2}^{T} = 1.5566\,\mathrm{ms}$ is multiplied by an increasing factor over the time. The factor increase began after 1 h to reduce the warm-up effect. Afterward, the factor is increased by 0.2 after 1000 measurements. The response delay $T_{2,3}^{R} = 1.5530\,\mathrm{ms}$ remains the same. In Fig. 4, the results of this experiment are presented. Fig. 4 (left) shows the raw distance measurements provided by the different ranging protocols. It can be observed that the noise of the CCSS-TWR case is rapidly increasing with a growing delay time. Moreover, the distance measurement of the SDS-TWR increases with a higher delay time. Fig. 4 (right) clearly shows that at the factor one, with equal response delays, the SDS-TWR equates the AltDS-TWR. At this point, the response times are nearly the same: $T_{1,2}^{T} \approx T_{2,3}^{R}$. The increase in the distance measurement of the CCSS-TWR was unexpected. This could be due to measurement imperfections of the clock drift error. Even if the remaining error was small, with increasing delay, it becomes more significant. The best results are provided by the AltDS-TWR protocol.

The AltDS-TWR protocol provides the best results, with a nearly constant distance measurement over time even with changing delay times. The only deviation from the ideal case appears at the beginning. This problem is highlighted in Fig. 5, where only the filtered distance measurements of the AltDS-TWR case are presented.

The linear approximation of the error is completely suitable for the clock drift correction. Furthermore, a position error caused by a constant velocity of the object is corrected by the linear interpolation because of the linear increase of the position error (pseudo clock drift). An acceleration high enough to cause an error greater than 5 mm would require almost 1000 g ($10^4\ \mathrm{m/s^2}$). Another possible explanation of the warm-up error could be the change in the reference frequency. In the case of the AltDS-TWR, the residual error depends only on the reference frequency and the time of flight $\epsilon_{\mathrm{AltDS}} = e_R T_{\mathrm{AltDS}}$. The DecaWave DW1000 chip of the EVK1000 is driven by an RSX-10 Rakon SMD crystal oscillator with a tolerance of 10 up to 50 ppm [24]. The short time of flight multiplied with the maximum change of the crystal oscillator offset is too small to cause a warm-up error of 3 cm. Therefore, the reason for the observed phenomenon is not the AltDS-TWR protocol.

C. Other Sources of Error

In practice, the timestamp of the DecaWave UWB device is affected by the signal power [14], [15] [see Fig. 6(a)]. Increasing the signal power causes a negative shift of the timestamp and vice versa. In [13], we showed how the signal power correction curve can be determined for each DecaWave

[1]The method used by the DW1000 firmware is misidentified as ADS-TWR in the TWR application note APS013 version 2.3 although it is in fact AltDS-TWR. This can be seen by comparison with [23, eq. (17)].

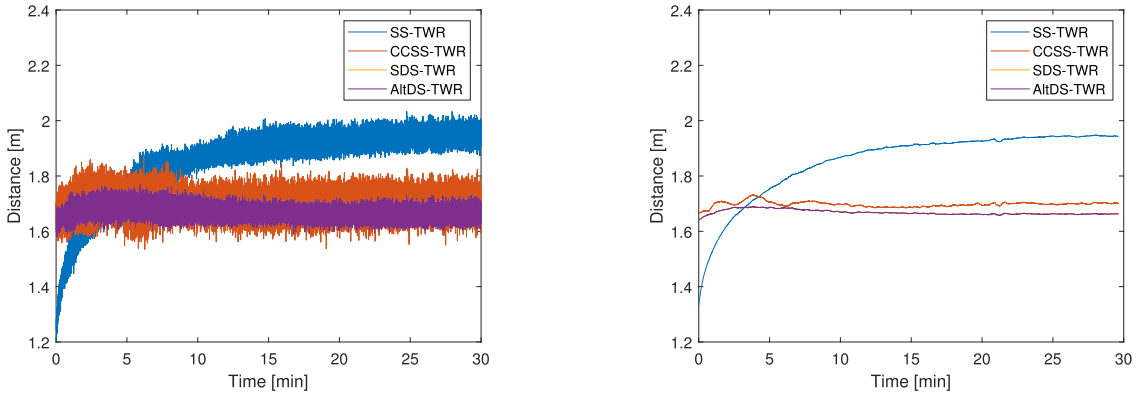

Fig. 3. Comparing the different TWR protocols. Distance measurements with respect to the time. (a) Raw distance measurements. (b) Filtered distance measurement.

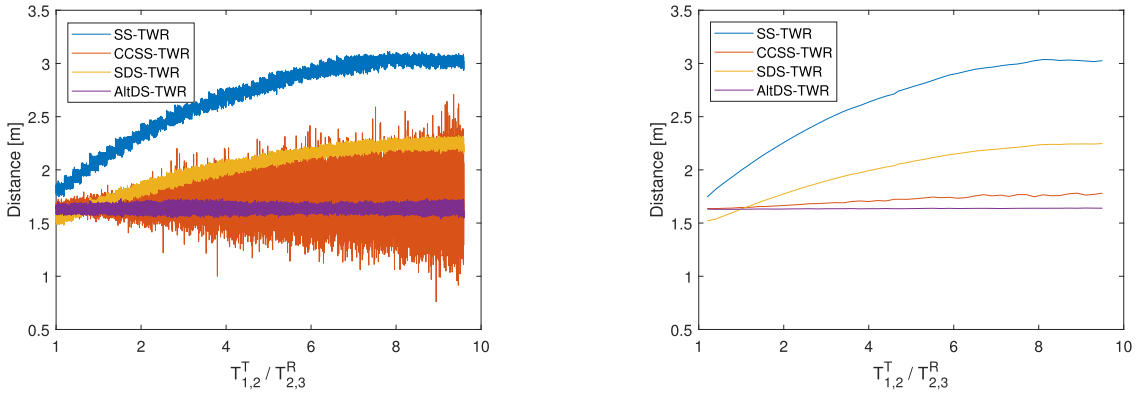

Fig. 4. Comparing the different TWR protocols with increasing response time. (a) Raw distance measurements with respect to response time ratio. (b) Filtered distance measurement with respect to response time ratio.

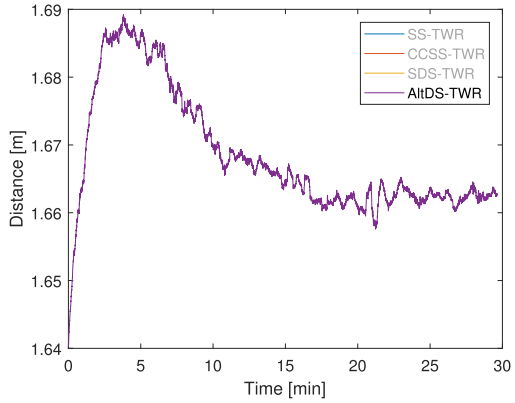

Fig. 5. Filtered distance measurement with respect to the time for the AltDS-TWR case. The plot is based on the measurement data from the first experiment.

UWB transceiver individually, without requiring additional measurement equipment. The developed algorithm is reducing the signal power to determine the dependence between the signal power and the timestamp shift. The presented technique allows us to correct the timestamp directly during the ranging procedure by considering the signal power correction terms E_1 and E_2. Note that the signal power may affect the tag and the reference station differently. At a lower signal power, the time difference $\Delta T^R_{1,2}$ increases.

The second important effect on the distance measurement is caused by the hardware delay. This time corresponds to the delay between the arrival of the signal on the antenna until the setting of the time stamp. The effect of the hardware delays A and B on the TWR [see Fig. 6(b)]. This error depends mainly on the temperature and can be estimated before the ranging [16].

The corrected time-of-flight equation (14) considers the effect of the signal power and the hardware delay for SS-TWR

$$\mathrm{TOF} = 0.5 \cdot \left(\Delta T^R_{1,2} - \Delta T^T_{1,2} - E_2 - E_1\right) - A - B. \quad (14)$$

IV. TDOA Measurement Technique

In applications with several moving targets (tags), TWR is less suitable due to its slow update rate. Trilateration in 2-D space requires at least three distance measurements. As the number of tags increases, the update rate decreases. In contrast to TOA, TDOA remains suitable for applications with large numbers of tags. In TDOA applications, the reference stations do not respond to the tags. Multilateration is performed by considering timestamp differences between anchors. Geometrically, TOA equations describe circles, whereas TDOA

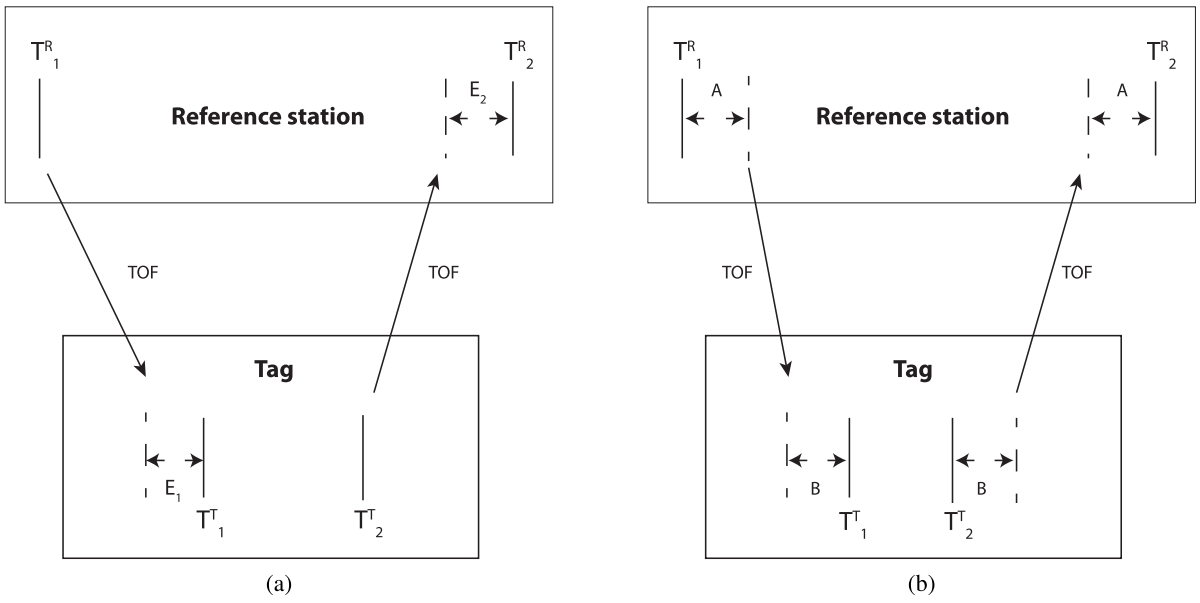

Fig. 6. Schematics for the TWR. (a) Effect of the power on the TOA. (b) Effect of the hardware delay on TOA.

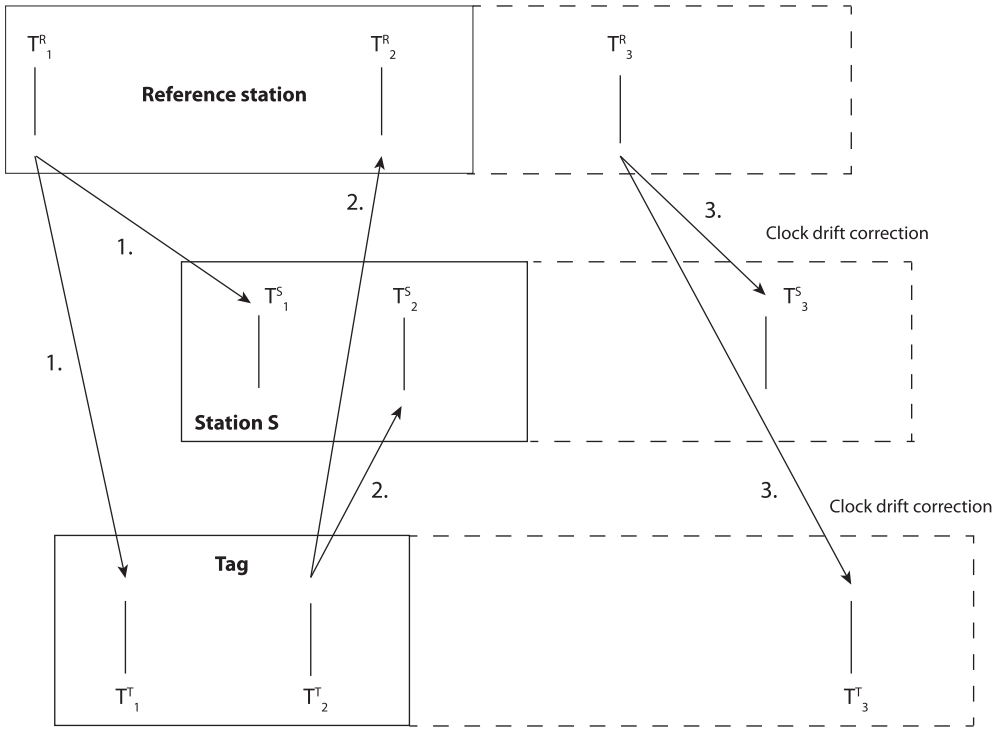

Fig. 7. TAO and TDOA ranging. The first two messages (1 and 2) are required for the ranging, and the third message (3) is for the clock drift correction. During the beginning of the ranging, the reference station sends the first message at its local time T_1^R. The tag and the passive station S receive the message and create timestamps T_1^S and T_1^T. In the next step, the tag sends a response message at its local time T_2^T . The reference station and station S receive this message at their local times T_2^R and T_2^S, respectively.

equations are hyperbolas in a 2-D space. Time synchronization between the BSs can be performed by wire [25] or with an additional station [3]. Various methods for wireless TDOA clock synchronization are presented in [26]–[28]. Without clock synchronization, it is necessary to correct the clock drift for the TDOA application. Dotlic *et al.* [17] used the CCSS-TWR method (see Section II-B) to correct the clock drift for TOA and TDOA. They also suggested to extend the SS-TWR with TDOA.

The results in Section II indicate that the AltDS-TWR protocol is the best solution to correct the clock drift. This is the reason why we are going to upgrade the AltDS-TWR protocol for the TDOA application. The error caused by signal power and the influence of the hardware delay are different

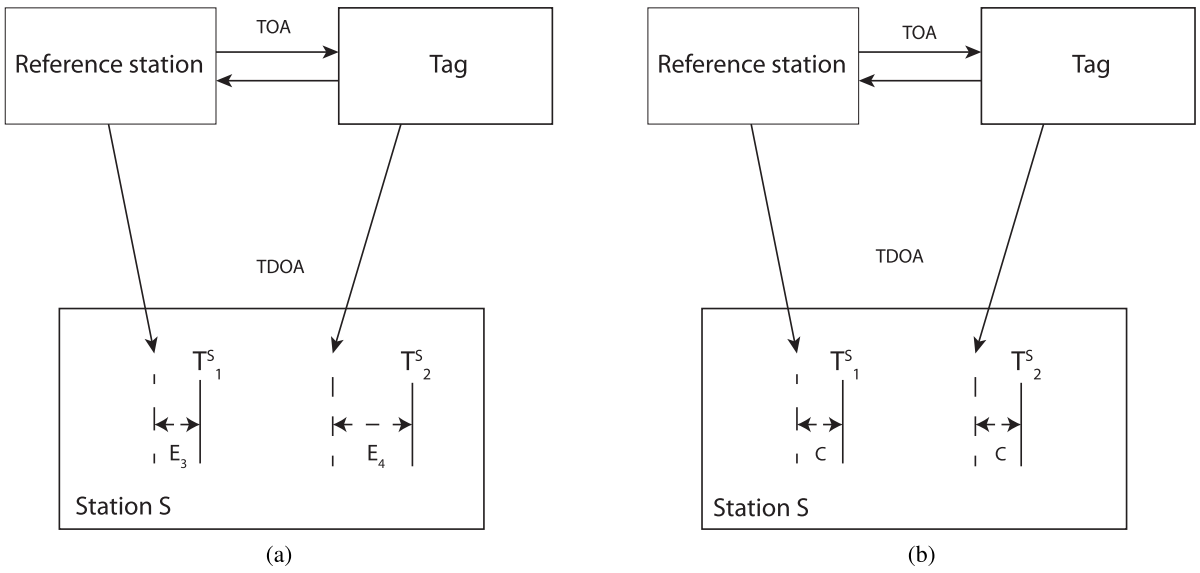

Fig. 8. (a) Effect of signal power on TDOA ranging. (b) Effect of the hardware offset. on the TDOA.

for the TDOA application compared with the TOA application. Both errors have been neglected in Section III but will now be corrected. In previous publications, the signal power error was corrected after obtaining the distance measurement. Using our presented method in [13], it is now possible to obtain the connection between the signal power and the timestamp shift. This allows us to correct the influence of the signal power as a part of the ranging protocol. First of all, the AltDS-TWR equation (10) is transformed into a more intuitive equation (17); it clearly shows that the clock drift error is corrected by linear interpolation. The time differences $T^T_{2,3}$ and $T^R_{2,3}$ are replaced by $(\Delta T^T_{1,3} - \Delta T^T_{1,2})$ and $(\Delta T^R_{1,3} - \Delta T^R_{1,2})$, respectively. The AltDS-TWR equation (10) becomes

$$T_{\text{AltDS}} = \frac{\Delta T^R_{1,2} \cdot \left(\Delta T^T_{1,3} - \Delta T^T_{1,2}\right)}{\Delta T^T_{1,3}} - \frac{\Delta T^T_{1,2} \cdot \left(\Delta T^R_{1,3} - \Delta T^R_{1,2}\right)}{\Delta T^T_{1,3}}. \quad (15)$$

This equation is transformed into the following equation:

$$T_{\text{AltDS}} = \Delta T^R_{1,2} - \frac{\Delta T^R_{1,2} \cdot \Delta T^T_{1,2}}{\Delta T^T_{1,3}} - \frac{\Delta T^T_{1,2} \cdot \left(\Delta T^R_{1,3} - \Delta T^R_{1,2}\right)}{\Delta T^T_{1,3}}. \quad (16)$$

Without the signal power error and the hardware delay, the function for the time-of-flight T_{TOF} calculation between two stations becomes

$$T_{\text{AltDS}} = 0.5 \cdot \left(\Delta T^R_{1,2} - \Delta T^T_{1,2}\left(\frac{\Delta T^R_{1,3}}{\Delta T^T_{1,3}}\right)\right). \quad (17)$$

With all the correction terms, (17) corresponds to

$$T_{\text{TOF}} = 0.5 \cdot \left(\Delta T^R_{1,2} - \left(\Delta T^T_{1,2} + E_1\right)\left(\frac{\Delta T^R_{1,3}}{\Delta T^T_{1,3}}\right) - E_2\right) - A - B. \quad (18)$$

Fig. 7 shows the protocol for the TOA-TDOA ranging, without the influence of the signal power and the hardware delay. The first two messages (1 and 2) are required for the ranging, and the third message (3) is for the clock drift correction. During the beginning of the ranging, the reference station sends the first message at its local time T^R_1; this station is used for the time synchronization and the clock drift correction. The tag and the passive station S receive the message and create timestamps T^S_1 and T^T_1. In the TDOA application, the stations S are the reference stations, which are located at known positions. In the next step, the tag sends a response message at its local time T^T_2. The reference station and station S receive this message at their local times T^R_2 and T^S_2, respectively. Without the influence of clock drift, hardware delay, and signal power, TOA equates $T_{\text{TOF}} = 0.5 \cdot (\Delta T^R_{1,2} - \Delta T^T_{1,2})$ and TDOA equation $T_{\text{TDOA}_K} = \Delta T^S_{1,2} - K$. The unknown parameter K is the time offset between the transmission times of messages 1 and 2. If both messages are emitted at the same time, this offset is zero. Similar to the AltDS-TWR, the third message is used for the clock drift correction. The reference station at its local time T^R_3 emits a message that is received by the tag and station S at T^S_3 and T^T_3, respectively. This leads to the clock drift corrected equations

$$T_{\text{TOF}} = 0.5 \cdot \left(\Delta T^R_{1,2} - \Delta T^T_{1,2}\left(\frac{\Delta T^R_{1,3}}{\Delta T^T_{1,3}}\right)\right)$$

and

$$T_{\text{TDOA}_K} = \Delta T^S_{1,2}\left(\frac{\Delta T^R_{1,3}}{\Delta T^S_{1,3}}\right) - K.$$

The influence of the signal power E_3 and E_4 and the hardware delay C for TDOA compared to TOA is shown in Fig. 8. The error caused by the signal power on the measurement is smaller for TDOA; this is because both timestamps of station S are affected. The hardware delay can be assumed to be constant between receiving messages 1 and 2, and hence, it has no effect on the time difference $\Delta T^S_{1,2}$.

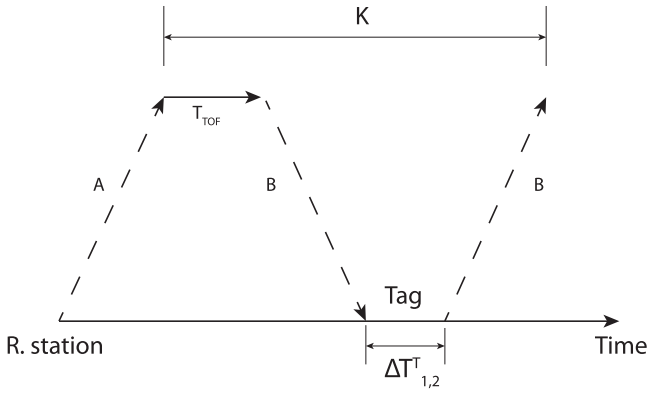

Fig. 9. Calculation of the offset K. A: delay caused by the hardware of the reference station (T_{TOA}: time of flight between the reference station and the tag). B: delay caused by the hardware of the tag ($\Delta T^T_{1,2}$: response time of the tag).

Considering the clock drift, signal power, and hardware delay leads to the TDOA equation

$$T_{\text{TDOA}_K} = \left(\Delta T^S_{1,2} + E_3 - E_4\right)\left(\frac{\Delta T^R_{1,3}}{\Delta T^S_{1,3}}\right) - K. \tag{19}$$

This time still depends on the offset K, as shown in Fig. 9. In general, this offset is simply the time of flight T_{TOF} of message 1 from the reference station to the tag plus the computation time $\Delta T^T_{1,2}$ at the tag before the signal 2 is emitted. The hardware delay A of the reference station does not affect the offset K because only the moment the signal leaves the transceiver matters. However, it is important to consider the hardware delay B of the tag two times: when the tag receives message 1 and when message 2 is emitted. At both times, the message is delayed by B.

It may be calculated as stated in the following equation:

$$K = T_{\text{TOF}} + \left(\Delta T^T_{1,2} + E_1\right)\left(\frac{\Delta T^R_{1,3}}{\Delta T^T_{1,3}}\right) + 2B. \tag{20}$$

The new TDOA equation after eliminating the offset K and including all corrections is shown in the following equation:

$$T_{\text{TDOA}} = \Delta T^R_{1,3}\left(\frac{\Delta T^S_{1,2} + E_3 - E_4}{\Delta T^S_{1,3}} - \frac{0.5\cdot\left(\Delta T^T_{1,2} + E_1\right)}{\Delta T^T_{1,3}}\right) - 0.5\cdot\left(\Delta T^R_{1,2} - E_2\right) + A - B. \tag{21}$$

V. Experimental Results: TOA and TDOA Position Estimation

The aim of this section is to apply the knowledge from Sections II–IV to estimate the unknown position of the tag with respect to several BSs at known positions. The experiments have been carried out only for the 2-D variant. The hardware delay as well as the signal power correction curve has been obtained before the multilateration. The real measurements have been performed with the DecaWave EVK1000. This device supports different message types, which are specified for the discovery phase, ranging phase, and final data transmission. Depending on the update rate and the preamble length, each message can vary from 190 to 3.4 ms. In our experiments, we only used 190-μs messages; the settings are listed in Table II.

TABLE II
Test Settings

Option	Value
Channel	2
Center Frequency	3993.6 MHz
Bandwidth	499.2 MHz
Pulse repetition frequency	64 MHz
Preamble length	128
Data rate	6.81 Mbps

Fig. 10. Constellation of the stations.

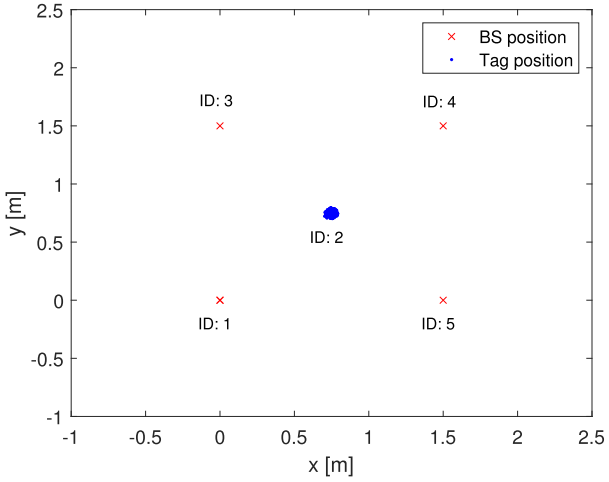

Fig. 11. TOA position estimation. The red crosses are the BSs. The blue dots are the results of the tag position estimations.

Fig. 10 and Table III show the constellation of the stations. The ground-truth data were obtained by laser distance measurements. The position of the tag with ID 2 is assumed to be unknown. The other stations with IDs 1, 3, 4, and 5 are

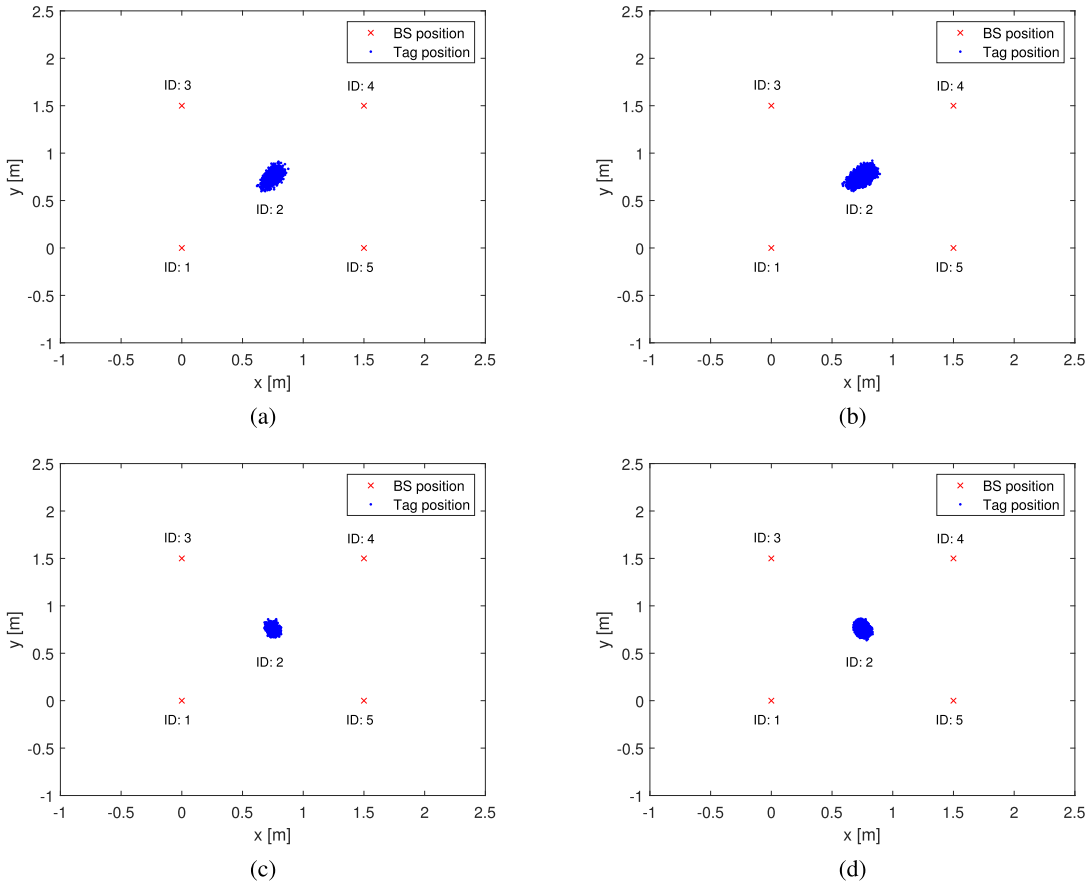

Fig. 12. TDOA position estimation. The red crosses are the BSs. The blue dots are the results of the tag position estimations. (a) Position estimations obtained with offset K and without TOA fusion. (b) Position estimations obtained without offset K optimization and without TOA fusion. (c) Position estimations obtained with offset K and with TOA fusion. (d) Position estimations obtained without offset K optimization and with TOA fusion.

TABLE III
POSITION OF THE STATIONS OBTAINED BY LASER DISTANCE MEASUREMENTS

Station ID	X-Axis [m]	Y-Axis [m]
1	0	0
2	0.75	0.75
3	0	1.5
4	1.5	1.5
5	1.5	0

TABLE IV
TDOA VARIANTS

TDOA variants	Definition
M_K	With K and without TOA fusion
M	Without K and without TOA fusion
$M_{K,F}$	With K and with TOA fusion
M_F	Without K and with TOA fusion

used to estimate the position of this tag. The station identified as the reference station changes during TWR. This is because the distances between the tag and the other stations must be calculated before the lateration. Unlike TOA, the reference station remains the same for TDOA; in this example, it is the reference station with ID 1. This characteristic of the TDOA measurement technique and the fact that stations S remain passive leads to a much higher update rate compared with TOA trilateration.

Given the corrected time measurements and the propagation speed of the signal, positioning may be performed to deduce the position of the tag with respect to the anchors.

A. TOA Lateration

In Fig. 11, the results of 2211 tag position estimations are presented; these results are provided by the TOA measurement technique. The BSs are illustrated by red crosses and the estimated tag positions by blue dots.

The TOA precision equals $(\sigma_x^2 + \sigma_y^2)^{1/2} = 0.0221$.

B. TDOA Multilateration

Section IV introduces our TDOA ranging protocol. It has the ability to correct the impact of the signal power and the hardware delay for every station individually. It is also possible to obtain the TOF between the reference station and the tag. The variants where the TDOA measurements are combined with the additional TOF measurement will be called "TOA fusion." The offset K can be determined either analytically [see (20)] or included in the numerical optimization. The latter will be denoted with the subscript K. This results in four variants, which are defined in Table IV.

The same geometric constellation of the BSs and the tag used in the TOA experiments in Section V-A is used here.

Fig. 12 shows the results of 12 587 tag position estimations provided by the TDOA measurements with and without offset K and TOA fusion. The BSs are illustrated by red crosses and the estimated tag positions by blue dots. The number of TDOA position estimations is much higher than that of TOA lateration (see Section V-A) due to the higher update rate. The covariance of the results for the different variants equals

$$\mathrm{Cov}(M_K) = \begin{pmatrix} 0.0015 & 0.0010 \\ 0.0010 & 0.0027 \end{pmatrix}$$
$$\mathrm{Cov}(M) = \begin{pmatrix} 0.0018 & 0.0011 \\ 0.0011 & 0.0020 \end{pmatrix}$$
$$\mathrm{Cov}(M_{K,F}) = \begin{pmatrix} 0.0005 & -0.0002 \\ -0.0002 & 0.0009 \end{pmatrix}$$
$$\mathrm{Cov}(M_F) = \begin{pmatrix} 0.0005 & -0.0002 \\ -0.0002 & 0.0006 \end{pmatrix}$$

and the precision

TDOA variants:	M_K	M	$M_{K,F}$	M_F
Precision:	0.0644	0.0610	0.0376	0.0336.

In contrast to station 4, the distance from stations 5 and 3 to the reference station is the same. The asymmetry of the position errors in M_K and M is expected due to station 1 being the reference station. The influence can be reduced by taking the additional distance measurement into account as shown in $M_{K,F}$ and M_F. For more information on the influence of geometry on positioning, also known as dilution of precision (DOP), see [29]. Furthermore, the ratio between the number of equations with respect to the unknown variables increasing is due to the TOA fusion, and hence, the overall noise is reduced. It can be observed that the best results are obtained for the variant M_F with TOA fusion and with an analytical determination of K. The difference from the case M_K without TOA fusion and with offset K optimization is 3 cm. The difference from the variants to each other, M_K to $M_{K,F}$ and M to M_F compared with M_K to M and $M_{K,F}$ to M_F, shows that the TOA fusion has the highest impact on precision. The standard deviation for the best TDOA case M_F is 1 cm higher than that in the TOA lateration (see Section V-A). It can be observed that the TOA measurements have a better precision compared with TDOA multilateration but a much slower update rate. This difference becomes even higher with more stations.

VI. Conclusion

This article analyzed the most common TWR protocols for the DecaWave UWB system, with the aim to find the one most suitable for correcting the clock drift error. These protocols were evaluated experimentally for their ability to correct the clock drift between the reference station and the tag. It was shown that the AltDS-TWR provides the best results. This protocol was expanded by the ability to correct the signal power and hardware delay for every station individually. The AltDS-TWR equation was transformed to perform the TDOA multilateration with four variants. It was shown that the effect of signal power and hardware delay for the TDOA case has to be considered differently. The best results were obtained with our new approach, where the offset K is computed analytically and fused with an additional distance measured. This method provides almost the same precision as TOA with the high update rate of TDOA. We are very confident that this new method will become the method of choice for DecaWave TDOA positioning.

Acknowledgment

The authors would like to thank Dr. Dimitri Bulatov from the Fraunhofer Institute of Optronics, System Technologies and Image Exploitation IOSB for his constructive criticism of the manuscript.

References

[1] D. Douglass and K. Monahan, *GPS Instant Navigation: A Practical Guide From Basics to Advanced Techniques by Kevin Monahan*. Portland, OR, USA: Fineedge.Com Llc, 1998.

[2] R. B. Thompson, "Global positioning system: The mathematics of GPS receivers," *Math. Mag.*, vol. 71, pp. 260–269, Oct. 1998.

[3] A. Resch, R. Pfeil, M. Wegener, and A. Stelzer, "Review of the LPM local positioning measurement system," in *Proc. Int. Conf. Localization GNSS*, Jun. 2012, pp. 1–5.

[4] X. Shen, S. Yang, J. He, and Z. Huang, "Improved localization algorithm based on RSSI in low power Bluetooth network," in *Proc. 2nd Int. Conf. Cloud Comput. Internet Things (CCIOT)*, Oct. 2016, pp. 134–137.

[5] L. Zwirello, T. Schipper, M. Jalilvand, and T. Zwick, "Realization limits of impulse-based localization system for large-scale indoor applications," *IEEE Trans. Instrum. Meas.*, vol. 64, no. 1, pp. 39–51, Jan. 2015.

[6] D. L. Adamy, *EW 102: A Second Course in Electronic Warfare*. Boston, MA, USA: Artech House, Jul. 2004.

[7] Y. Zhou, C. L. Law, Y. L. Guan, and F. Chin, "Indoor elliptical localization based on asynchronous UWB range measurement," *IEEE Trans. Instrum. Meas.*, vol. 60, no. 1, pp. 248–257, Jan. 2011.

[8] I. Dotlic, A. Connell, H. Ma, J. Clancy, and M. McLaughlin, "Angle of arrival estimation using decawave DW1000 integrated circuits," in *Proc. 14th Workshop Positioning, Navigat. Commun. (WPNC)*, Oct. 2017, pp. 1–6.

[9] J. F. M. Gerrits, J. R. Farserotu, and J. R. Long, "Multipath behavior of FM-UWB signals," in *Proc. IEEE Int. Conf. Ultra-Wideband*, Sep. 2007, pp. 162–167.

[10] S. K. Rashid A. Saeed, "Ultra-wideband (UWB) geolocation in NLOS multipath fading environments," in *Proc. 13th IEEE Int. Conf. Netw. Jointly held with IEEE 7th Malaysia Int. Conf Communic*, Nov. 2005, p. 6.

[11] A. R. Jimenez Ruiz and F. Seco Granja, "Comparing ubisense, BeSpoon, and DecaWave UWB location systems: Indoor performance analysis," *IEEE Trans. Instrum. Meas.*, vol. 66, no. 8, pp. 2106–2117, Aug. 2017.

[12] M. Haluza and J. Vesely, "Analysis of signals from the DecaWave TREK1000 wideband positioning system using AKRS system," in *Proc. Int. Conf. Mil. Technol. (ICMT)*, May 2017, pp. 424–429.

[13] J. Sidorenko, V. Schatz, M. Arens, N. Scherer-Negenborn, and U. Hugentobler, "Decawave UWB clock drift correction and power self-calibration," *Sensors*, vol. 19, p. 2942, Jan. 2019.

[14] *DW1000 User Manual, Version 2.15*. Accessed: Sep. 4, 2019. [Online]. Available: https://www.decawave.com

[15] *Decawave APS011 APPLICATION NOTE: Sources of error in TWR, Version 1.0*. Accessed: Sep. 4, 2019. [Online]. Available: https://www.decawave.com

[16] *Decawave APS014 APPLICATION NOTE: Antenna delay calibration DW1000-Based Products and Systems, Version 1.2*. Accessed: Sep. 4, 2019. [Online]. Available: https://www.decawave.com

[17] I. Dotlic, A. Connell, and M. McLaughlin, "Ranging methods utilizing carrier frequency offset estimation," in *Proc. 15th Workshop Positioning, Navigat. Commun. (WPNC)*, Oct. 2018, pp. 1–6.

[18] N. I. Fofana, A. van den Bossche, R. Dalcé, and T. Val, "An original correction method for indoor ultra wide band rangingbased localisation system," in *Ad-hoc, Mobile, and Wireless Networks* (Lecture Notes in Computer Science), vol. 9724. Cham, Switzerland: Springer, pp. 79–92, Jun. 2016.

[19] A. van den Bossche, R. Dalce, I. Fofana, and T. Val, "DecaDuino: An open framework for wireless time-of-flight ranging systems," in *Proc. Wireless Days (WD)*, Mar. 2016, pp. 1–7.

[20] F. M. Martel, J. Sidorenko, C. Bodensteiner, and M. Arens, "Augmented reality and UWB technology fusion: Localization of objects with head mounted displays," in *Proc. 31st Int. Tech. Meeting Satell. Division Inst. Navigat. (ION GNSS+)*, Oct. 2018, pp. 685–692.
[21] R. Hach, (Jun. 2005). *Symmetric Double Sided Two-Way Ranging*. [Online]. Available: http://www.ieee802.org/15/pub/TG4a.html, doc: IEEE 15-05-0334-00-004a.
[22] Y. Jiang and V. C. M. Leung, "An asymmetric double sided two-way ranging for crystal offset," in *Proc. Int. Symp. Signals, Syst. Electron.*, Jul. 2007, pp. 525–528.
[23] D. Neirynck, E. Luk, and M. McLaughlin, "An alternative double-sided two-way ranging method," in *Proc. 13th Workshop Positioning, Navigat. Commun. (WPNC)*, Oct. 2016, pp. 1–4.
[24] *Product Manual RSX-10*. Accessed: Sep. 5, 2019. [Online]. Available: http://www.rakon.com
[25] *Decawave APS007 Application Note: Wired Synchronizsation of Anchor Nodes in a TDOA Real Time Location System, Version 1.0*, Accessed: Sep. 5, 2019. [Online]. Available: https://www.decawave.com
[26] C. McElroy, D. Neirynck, and M. McLaughlin, "Comparison of wireless clock synchronization algorithms for indoor location systems," in *Proc. IEEE Int. Conf. Commun. Workshops (ICC)*, Jun. 2014, pp. 157–162.
[27] V. Djaja-Josko and J. Kolakowski, "A new method for wireless synchronization and TDOA error reduction in UWB positioning system," in *Proc. 21st Int. Conf. Microw., Radar Wireless Commun. (MIKON)*, May 2016, pp. 1–4.
[28] J. Tiemann, F. Eckermann, and C. Wietfeld, "ATLAS—An open-source TDOA-based ultra-wideband localization system," in *Proc. Int. Conf. Indoor Positioning Indoor Navigat. (IPIN)*, Oct. 2016, pp. 1–6.
[29] N. Salman, H. K. Maheshwari, A. H. Kemp, and M. Ghogho, "Effects of anchor placement on mean-CRB for localization," in *Proc. 10th IFIP Annu. Medit. Ad Hoc Netw. Workshop*, Jun. 2011, pp. 115–118.
[30] J. Sidorenko, N. Scherer-Negenborn, M. Arens, and E. Michaelsen, "Improved linear direct solution for asynchronous radio network localization (RNL)," in *Proc. Inst. Navigat. ION Pacific PNT Meeting*, May 2017, pp. 376–382.

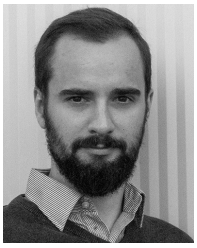

Juri Sidorenko received the Diploma degree in mechanical engineering from the Technical University of Braunschweig, Brunswick, Germany, in 2012, and the Master of Science degree from Cranfield University, Cranfield, U.K., in 2014. He is currently pursuing the Ph.D. degree in engineering with the Technical University of Munich, Munich, Germany.

He is currently a Research Assistant with the Fraunhofer Institute of Optronics, System Technologies and Image Exploitation IOSB, Ettlingen, Germany. His research interest includes the localization and self-calibration of sensor networks.

Volker Schatz received the Diploma degree in physics from Ruperto Carola University, Heidelberg, Germany, in 2000, with a focus on the development of trigger circuits for high-energy physics experiments, and the Ph.D. degree theoretical particle physics from Heidelberg University, Heidelberg, in 2003.

After a year of post-doctoral research in theoretical geophysics, he started work at the Fraunhofer Institute of Optronics, System Technologies and Image Exploitation IOSB, Ettlingen, Germany, in 2005. His current occupations and research interests are developing multisensor data acquisition systems, synchronizing imaging sensors for sensor fusion applications, and measuring the timing behavior of commercial cameras.

Norbert Scherer-Negenborn received the Diploma and Ph.D. degrees in physics from the University of Freiburg, Breisgau, Germany, in 1996 and 2000, respectively.

He is currently the Group Leader of the Tracking and Tracking Assessment Group, Fraunhofer Institute for Optronics, System Technology and Image Exploitation IOSB, Ettlingen, Germany.

Michael Arens received the Diploma degree in computer science and the Ph.D. (Dr.rer.nat.) degree from the University of Karlsruhe, Karlsruhe, Germany, in 2001 and 2004, respectively.

He is currently the Head of the Department of the Object Recognition (OBJ), Fraunhofer Institute for Optronics, System Technology and Image Exploitation IOSB, Ettlingen, Germany.

Urs Hugentobler received the Ph.D. degree in astronomy from the University of Bern, Bern, Switzerland, in 1997. He studied theoretical physics at the University of Bern.

After working as a Post-Doctoral Researcher at the European Space Agency (ESA), Paris, France, he joined the GPS Research Group, University of Bern, as the Head, in 1999. He has headed the Department of Space Geodesy and the Space Geodesy Research Unit, TUM, since 2006. He is the Secretary-General of the Project Geodesy (DGK) of the Bavarian Academy of Science.